

INTERNALIZING WORLD MODELS VIA SELF-PLAY FINETUNING FOR AGENTIC RL

Shiqi Chen^{*†}, Tongyao Zhu^{†7}, Zian Wang^{†8}, Jinghan Zhang^{†3}, Kangrui Wang²,

Siyang Gao¹, Teng Xiao^{†5,6}, Yee Whye Teh⁴, Junxian He^{*3}, Manling Li^{*2}

¹City University of Hong Kong, ²Northwestern University,

³The Hong Kong University of Science and Technology, ⁴Oxford University, ⁵Allen Institute for AI (AI2),

⁶University of Washington, ⁷National University of Singapore, ⁸The Hong Kong Polytechnic University

<https://github.com/shiqichen17/SPA>

ABSTRACT

Large Language Models (LLMs) as agents often struggle in *out-of-distribution* (*OOD*) scenarios. Real-world environments are complex and dynamic, governed by task-specific rules and stochasticity, which makes it difficult for LLMs to ground their internal knowledge in those dynamics. Under such *OOD* conditions, vanilla RL training often fails to scale; we observe *Pass@k*—the probability that at least one of k sampled trajectories succeeds—drops markedly across training steps, indicating brittle exploration and limited generalization. Inspired by model-based reinforcement learning, we hypothesize that equipping LLM agents with an internal world model can better align reasoning with environmental dynamics and improve decision-making. We show how to encode this world model by decomposing it into two components: state representation and transition modeling. Building on this, we introduce SPA, a simple reinforcement learning framework that cold-starts the policy via a Self-Play supervised finetuning (SFT) stage to learn the world model by interacting with the environment, then uses it to simulate future states prior to policy optimization. This simple initialization outperforms the online world-modeling baseline and greatly boosts the RL-based agent training performance. Experiments across diverse environments like Sokoban, FrozenLake, and Sudoku show that our approach significantly improves performance. For example, SPA boosts the Sokoban success rate from **25.6%** to **59.8%** and raises the FrozenLake score from **22.1%** to **70.9%** for the Qwen2.5-1.5B-Instruct model.

1 INTRODUCTION

Agentic reinforcement learning (RL) has become a primary framework for finetuning Large Language Model (LLM) agents (Wang et al., 2025b; Jin et al., 2025). Using ReAct-style scaffolds (Yao et al., 2023) for environmental interaction and optimizing for task rewards, this approach has been successfully applied to computer-use planning (Cao et al., 2025), tool use (Schick et al., 2023), and web search (Wu et al., 2025; Jin et al., 2025). However, the performance degrades sharply in out-of-distribution (*OOD*) environments that are beyond the LLM’s pre-training distribution. Under such cases, the state is unfamiliar to the policy model, leading to low relative likelihood—quantified by combining the perplexity (PPL) of state descriptions and state space. As shown in Table 1, Sokoban, FrozenLake, and Sudoku exhibit state PPLs far above the Random-Guess PPL under these environments, yet ALFWorld and WebShop yield much lower state PPLs compared with the Random-Guess PPL, indicating a stronger distributional shift in the former environments.

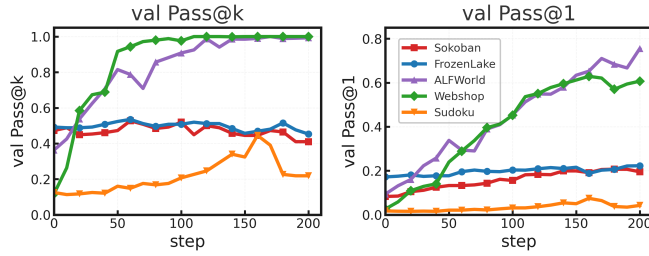


Figure 1: Validation score on five environments. Sokoban, FrozenLake and Sudoku are OOD for the models, where *Pass@k* ($k=8$) drops with training. However, in ALFWorld and WebShop, *Pass@k* increases greatly with training.

^{*}Corresponding Author

[†]Core Contributor

To diagnose when LLM agents struggle to learn in OOD environments, we empirically investigate agent performance during RL fine-tuning and uncover a systematic divergence between two key metrics: *Pass@1*, which measures the success rate of the agent’s highest-probability trajectory, and *Pass@k*, which measures the success rate across k sampled trajectories, reflecting the ability to cover diverse correct solutions across multiple trajectories. As shown in Figure 1, in OOD environments like Sokoban, FrozenLake, and Sudoku, standard RL training causes *Pass@k* performance to consistently degrade, while *Pass@1* increases marginally. This is different from in-domain settings (e.g., ALF-World and Webshop), where both metrics sharply improve. This divergence reveals a fundamental limitation: current agentic RL develops a narrow, exploitative solution path (reflected in *Pass@1*), but fail to generalize across multiple solution paths (reflected in *Pass@k*). The agents can “get better at one path” but cannot build the broader world knowledge required for robust generalization in unfamiliar OOD environments. To this end, we ask an important research question: *How can we achieve effective and efficient agentic reinforcement learning in OOD environments?*

In this paper, we answer this question affirmatively. We propose SPA (Self Play Agent), a simple yet effective framework that enables agents to first self-play to acquire world knowledge of an OOD environment, and then exploit this knowledge to act effectively. We argue that the key to unlocking generalization of unfamiliar OOD environments is for an agent to internalize a **world model** of the environment’s underlying rules, recognizing the current state and reasoning about how actions transform it to the next state over time. We refer to this structured understanding as a world model following Xing et al. (2025). The benefits of explicit world models are well-established in classical non-LLM-based RL in (Janner et al., 2019; Yu et al., 2020), where they enhance planning and sample efficiency. We hypothesize that LLM agents can benefit in an analogous way: if the model can simulate how one state changes after one action, it can reason about long action sequences in OOD environments. **World modeling enables agents to ground their reasoning in the rules of the environment rather than memorized trajectories.** However, the question of how to effectively and scalably acquire such world models for LLM agents remains open.

Our central claim is that self-play finetuning is a more effective and scalable vehicle for injecting world-model knowledge than online RL methods that inject it via reward shaping (Wang et al., 2025a). Driven by task-specific rewards, online RL is exploitative by forcing the agent to quickly narrow its policy and overfit to the first successful trajectory, improving *Pass@1*. Our key finding is **exploration before exploitation**: Self-play finetuning allows the agent to form a robust internal world model by exploring the environment’s state space and action space, rather than overfitting reward quirks. This coverage yields a reusable scaffold that diversifies multistep reasoning and raises *Pass@k*.

An effective self-play finetuning, as designed in SPA, focuses on exploration on both state space and action space: **1) State Estimation.** To explore the state space s_t , the goal is to transform unfamiliar states to familiar ones through systematic exposure. When agents encounter states with high perplexity under the model’s state encoder, this signals novelty and triggers agents to seek exploration via self-play and update their understanding/belief, gradually reducing their perplexity. **2) Transition Modeling.** Exploration of the action space means making the environment’s transitions predictable with an accurate transition kernel $p_\theta(s_{t+1} | s_t, a_t)$. Effective self-play generates diverse experience triples (s_t, a_t, s_{t+1}) to jointly fit the state encoder and transition predictor *without* relying on dense external rewards. With the learned kernel, the reachable set under k stochastic rollouts expands, directly lifting *Pass@k* even when *Pass@1* remains low.

Putting these together, SPA scales improvements in RL: both *Pass@1* and *Pass@k* grow over training. Moreover, *Pass@k* becomes an agentic metric, capturing whether an agent leverages a learned world model to diversify attempts and succeed within a small rollout budget, while avoiding the reward overfitting and credit-assignment brittleness common in online RL. We evaluate SPA on two well-studied grid worlds, *Sokoban* and *FrozenLake*, and a math-reasoning environment, *Sudoku*. These tasks demand multistep spatial reasoning and precise action control. Under a fixed compute budget of 1000 training steps, our method lifts average success rates on *Sokoban* from 25.6% to 59.8% and on *FrozenLake* from 22.1% to 70.9% as shown in Figure 2. Qualitative case studies further show that the internal world model induces more deliberate, globally consistent plans that benefit subsequent RL.

2 WORLD MODELING: JOINTLY OPTIMIZING STATES AND DYNAMICS

In this section, we introduce SPA, a simple and effective framework for improving LLM agent training. We show the framework in Figure 3. The central idea is to strengthen grounding through explicit world modeling prior to policy learning. Specifically, we decompose world modeling into two

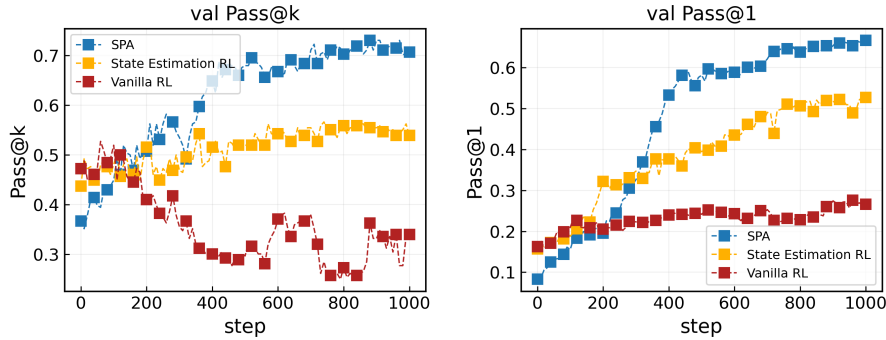


Figure 2: Validation performance on Sokoban and Frozen Lake. Red: Vanilla RL(StarPO baseline); Yellow: state-estimation RL; Blue: SPA (world-modeling SFT as a cold start, then state-estimation RL). Left: *Pass@k*; Right: *Pass@1*.

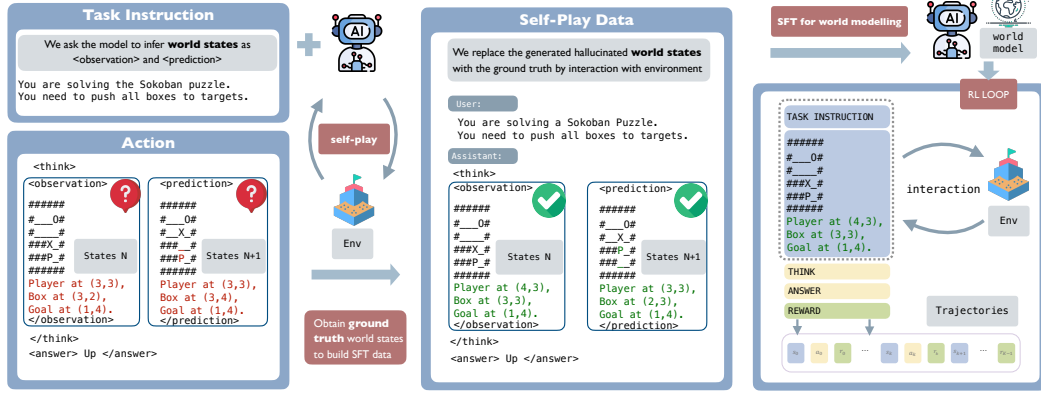


Figure 3: SPA equips an LLM agent with an inner world model. The world model is decomposed into two parts: (i) State Estimation, which converts raw observations into structured, informative natural-language descriptions of the world state; and (ii) Transition Modeling, trained in a self-play Supervised Fine-Tuning setting to predict next-state representations from current states.

components: *state representation* and *transition dynamics*. By jointly modeling states and transition dynamics, the agent is regularized to follow structured state descriptions while interacting with the environment, thereby improving grounding. We train the world model via supervised finetuning on transition dynamics and use it to initialize policy learning. Our method does not rely on external knowledge or larger teacher models; instead, it learns entirely from the base model’s own experience. In the following, we present the state-representation schema and the transition-modeling procedure.

2.1 OPTIMIZING STATE ESTIMATION

We hypothesize that a key source of difficulty in agent RL training is distribution shift: the observed states are out-of-domain with respect to the models pretraining data, making them hard to parse and reason about. In particular, LLM agents struggle to capture spatial relationships when the environment state is rendered as a symbolic text string rather than an explicit 2D layout: for instance, a 6*6 Sokoban board is represented as #####\n#####\n#_###\n#_###\n#_###\n#0_XP# in Wang et al. (2025b). However, when world states are expressed as raw symbols, LLMs may lose track of crucial elements, leading to unstable training. As shown in Table 1, we observe a high perplexity value of raw state representations, in environments with natural language descriptions

Table 1: Average PPL of state representations evaluated with Qwen2.5-Instruct-1.5B. #States denotes the number of possible values each grid cell can take (=random guess PPL). State Estimation significantly reduces PPL in text games.

Task	PPL	#States
Sokoban	163.9	7
+ State Estimation	19.6	
Frozen Lake	187.1	6
+ State Estimation	15.4	
Sudoku	15.5	5
+ State Estimation	7.3	
ALFWORLD	6.0	$ V $
WebShop	11.7	$ V $

Table 2: Results on Sokoban, FrozenLake and Sudoku for different models. (Metrics in $\times 10^{-2}$).

Model	Sokoban		FrozenLake		Sudoku	
	Pass@1	Pass@8	Pass@1	Pass@8	Pass@1	Pass@8
Qwen2.5-0.5B-Instruct	5.5	25.8	8.1	32.8	0.0	0.0
+Vanilla RL	16.9	35.9	22.8	30.1	0.0	0.0
+State Estimation RL	20.4	38.7	24.2	26.6	4.5	14.1
+VAGEN (Wang et al., 2025a)	33.3	44.9	25.8	40.6	0.1	0.8
+ SPA	36.7	45.3	46.9	65.6	18.2	43.8
Qwen2.5-1.5B-Instruct	16.3	47.3	17.2	49.2	1.6	11.3
+Vanilla RL	25.6	34.0	22.1	30.7	0.0	0.0
+State Estimation RL	52.7	53.9	27.6	34.8	39.1	72.3
+VAGEN (Wang et al., 2025a)	44.5	50.0	37.7	43.0	0.0	0.0
+ SPA	59.8	69.5	70.9	75.0	59.6	94.9
Qwen2.5-3B	12.5	35.9	6.9	26.9	0.0	0.0
+Vanilla RL	31.4	35.5	7.6	16.0	0.0	0.0
+State Estimation RL	26.2	27.7	24.7	35.5	24.1	26.2
+VAGEN (Wang et al., 2025a)	31.9	43.0	30.7	34.0	0.0	0.0
+ SPA	49.7	58.2	41.3	46.1	69.9	89.8
LLaMA3.2-1B-Instruct	8.3	33.2	10.2	41.0	0.0	0.0
+Vanilla RL	21.2	39.8	10.8	24.6	0.1	1.2
+State Estimation RL	31.6	44.1	19.3	29.7	45.0	71.1
+VAGEN (Wang et al., 2025a)	47.4	50.8	24.5	29.3	0.1	0.8
+ SPA	53.0	68.0	64.8	71.1	81.3	100
GPT-OSS-20B	45.8	84.4	68.8	100	61.8	100
+State Estimation	55.1	89.1	73.3	100	68.1	100

PPL. To address this, we choose to provide a better and natural format (denoted as b_t) to abstract the world state and concatenate it with the raw state (s'_t) to give a better representation. In text games, b_t represents the coordinates of the positions of key game components. For example, the player, boxes, and goals in the Sokoban game. We hypothesize that using natural language descriptions can reduce the reasoning complexity. Finally, our optimized state representation is $s_t = \text{Concat}(s'_t, b_t)$. The table below shows an example. Text highlighted in red denotes our additions to incorporate a better state representation. In Table 1, we also observe a significant reduction in perplexity. As shown in the *State Estimation RL* row of Table 2, we see the improved representation yields higher RL performance than vanilla RL baseline (listed in the *Vanilla RL* row). Though modest, these gains indicate that better state representations benefit both Pass@k and Pass@1. In the next subsection, we will introduce how we equip the agent with transition-dynamics modeling based on state estimation.

Sokoban Prompt: Symbol with Coordinates

```
You are solving the Sokoban puzzle.
You are the player and you need to push all boxes to targets. You are provided
with a symbol grid and the zero-indexed coordinates of the player, each box, and
each target. Coordinates range from the top-left corner (0, 0) to the
bottom-right corner (5, 5).
...
The meaning of each symbol in the state is:
#: wall, _: empty, 0: target, √: box on target, X: box, P: player, S: player on
target.
Your available actions are: Up, Down, Left, Right
...
Turn 1:
State:
#####
#___0#
#___#
####X_#

```

```
###P_#
#####
Player (P) is at (4,3); box (X) is at (3,3); target (0) is at (1,4).
...
```

2.2 INJECTING TRANSITION MODELING VIA SELF-PLAY FINE-TUNING

Based on the interpretable environment states, we inject transition dynamics into the LLM agent via a self-play finetuning process. It includes two stages: *trajectory collection via self-play* and *dynamics transition training*. During the trajectory collection stage, we use the base model to freely explore and interact with the environment under a self-play scenario to update the model’s belief of the world.

Self-Play Data Generation We collect the data by prompting the model to interact with the environment. This self-play interaction process with the environment is repeated over T turns to collect a trajectory $\tau = (s_0, o_0, a_0, r_0, \dots, s_{T-1}, o_{T-1}, a_{T-1}, r_{T-1}, s_T, o_T)$. At each step, the action a_t is parsed and executed. The environment then produces a reward r_t as feedback and transitions to a new state s_{t+1} , which provides the agent with a new observation o_{t+1} . The structure of a_t is designed to incorporate explicit visual state reasoning, with a particular focus on world modeling. To reason about world states, we require the model to think before taking actions: model generation $a_t = (z_t, \hat{a}_t)$ is a sequence of text including both reasoning tokens z_t and executable action \hat{a}_t . To incorporate world modeling into the trajectories, we prompt the LLM agent to describe the current state and predict the next state during reasoning (Wang et al., 2025a). Specifically, the reasoning variable z_t between `<think>` and `</think>` is required to explicitly represent both the current state and the predicted next state: `<think><observation> \hat{s}_t </observation><prediction> \hat{s}_{t+1} </prediction></think>` `<answer> \hat{a}_t </answer>`. Then, we replace the model’s beliefs about current states \hat{s}_t and future states \hat{s}_{t+1} with the ground-truth states s_t and s_{t+1} from the environment, resulting in the training trajectory: `<think><observation> s_t </observation><prediction> s_{t+1} </prediction></think>` `<answer> \hat{a}_t </answer>`. Next, we perform supervised finetuning (SFT) on these trajectories that reflect the environmental dynamics, enabling the model to learn the environment dynamics. The resulting SFT model serves as a strong initialization for downstream RL training. The prompts we use are listed under “Observation then Prediction prompts” in Appendix A.

World Modeling. With the constructed trajectory $\tau_{1:T}$ above, and let $\tau_{<i}$ denote the prefix up to token $i - 1$, we optimize a simple masked token-level cross-entropy over all tokens enclosed by the special tags to capture environmental dynamics and to internalize world models in agents.

$$\mathcal{L}_W(\theta) = -\frac{1}{\sum_{i=1}^T M_i} \sum_{i=1}^T M_i \log p_\theta(\tau_i \mid \tau_{<i}), \quad (1)$$

$$\text{where } M_i = \mathbb{1}_{[\tau_i \in (\text{span}(\text{<think>}, \text{</think>}) \cup \text{span}(\text{<answer>}, \text{</answer>}))]} \quad (2)$$

We explicitly represent both the prediction of the current state and the next state in the reasoning.

This simple world-modeling training objective is to enhance the agent’s grounding capability, improving its ability to generate effective next states and answers. Consequently, the tokens corresponding to the environment’s observations are masked out during the loss calculation. The resulting model serves as an effective initialization for downstream policy RL learning.

2.3 RL TRAINING

After obtaining a good world model by SFT, we do Reinforcement Learning to boost the policy model. We use the Proximal Policy Optimization (PPO) (Schulman et al., 2017) algorithm for RL. Denote τ as trajectory, $u_i(\theta) = \frac{\pi_\theta(\tau_i \mid \tau_{<i})}{\pi_{\text{old}}(\tau_i \mid \tau_{<i})}$ as the probability ratio between the current and old policies, and let $\tau_{<i}$ denote the prefix of token i . The PPO loss is defined as:

$$J^{\text{PPO}}(\theta) = \frac{1}{\sum_i M_i} \sum_i M_i \cdot \min(u_i(\theta) A_i, \text{clip}(u_i(\theta), 1 - \varepsilon, 1 + \varepsilon) A_i),$$

where M_i is a mask that is 1 for answer tokens and 0 for contextual tokens, A_i is the per-token advantage and ε is a clipping hyperparameter. This objective is to optimize the policy to gain more rewards. And here we use our optimized s_t (described in Section 2.1) to represent the world states to better encode the world knowledge during RL training.

3 EXPERIMENTS

Experiment setting and baselines We conduct experiments on a diverse set of models of varying sizes, including Qwen2.5-0.5B-Instruct, Qwen2.5-1.5B-Instruct, Qwen2.5-3B (Team, 2024) and LLaMA-3.2-1B-Instruct (Dubey et al., 2024). Our evaluation spans multiple environments, such as Sokoban, FrozenLake, and Sudoku. Our codebase is developed based on RAGEN (Wang et al., 2025b). These text-based game environments are highly controllable; we adjust task difficulty by varying grid size to match model capacity. For Sokoban, we fix a 6×6 grid for all models. For FrozenLake, we use 4×4 for smaller models (Qwen2.5-0.5B-Instruct, Qwen2.5-1.5B-Instruct and LLaMA-3.2-1B-Instruct) and 6×6 for Qwen2.5-3B to avoid ceiling effects observed with the 4×4 setting. For Sudoku, we use a 4×4 grid with six empty cells to be filled. We train with a batch size of 32 and collect eight rollouts per environment at each update step. For evaluation, we use both Pass@8 and Pass@1 metrics. We use VAGEN (Wang et al., 2025a) as our baseline. This method enables online world-model learning during RL by providing observation and prediction-based reward signals. We also evaluate a SOTA model: open-source GPT-OSS-20B (OpenAI, 2025).

Small models could outperform strong models on text games with SPA. Our main results are shown in Table 2. For every model we evaluated, SPA consistently outperforms State Estimation RL, which in turn outperforms vanilla RL. For instance, for Qwen2.5-1.5B-Instruct, SPA could obtain 59.8 Pass@1 score after 1000 training steps for Sokoban environment, and 70.9 Pass@1 for FrozenLake environment, which even outperforms GPT-OSS-20B model. Across other models, Qwen2.5-0.5B-Instruct and Qwen2.5-3B, SPA delivers substantial improvements over baseline methods on all our evaluated environments. This suggests our approach effectively drives exploration and consolidates environment knowledge in OOD scenarios.

SPA outperforms the reward-based method VAGEN. VAGEN (Wang et al., 2025a) performs world modeling by eliciting current-state observations and predicting next states, and then applies a reward to encourage accurate grounding. For a fair comparison, we reimplemented VAGEN in the same state-estimation setting as SPA. Empirically, VAGEN attains performance comparable to the Abstraction PPO baseline and yields little improvement on our testbed. In contrast, SPA delivers substantial gains. We hypothesize that this advantage stems from SPA confining world-model learning to the Supervised Fine-Tuning (SFT) stage and optimizing only the accuracy objective during RL training, thereby avoiding the multi-objective interference introduced by VAGEN. Across benchmarks, SPA consistently surpasses VAGEN, suggesting that the accuracy objective is brittle and should not be perturbed during RL training.

4 WHAT CONTRIBUTES TO SUCCESSFUL WORLD MODELLING?

We further disentangle the contributions of transition-model learning, grounded state representations, and multi-turn RL interaction to analyze why SPA succeeds. Our analysis highlights four critical factors: (i) *transition modeling*, which distills environment dynamics and sharpens credit assignment; (ii) *grounded state representations*, which make spatial relations explicit and enable reliable perception-action coupling; (iii) *a strong policy for world-model interaction*, which drives meaningful exploration; and (iv) *sufficient world-modeling data*, which ensures adequate coverage of the environment’s dynamics. In addition, we find that multi-turn RL broadens the reasoning frontier by introducing exploration-exploitation dynamics absent in prior single-turn settings.

4.1 EFFECT OF TRANSITION MODELLING

Transition-model learning is key to RL scaling. Masking the SFT loss on the current and next states results in no improvement. To isolate the effect of world modeling supervision, we remove explicit transition (world modeling) annotations (*observation* and *prediction* spans) from the SFT corpus and replace them with a masking token `[MASKED]` and set the masking tokens’ loss to 0 during SFT. Starting from the base pretrained model, we run SFT on this masked data and use the resulting checkpoint to initialize the PPO stage. We show the results in Figure 4. In the masked

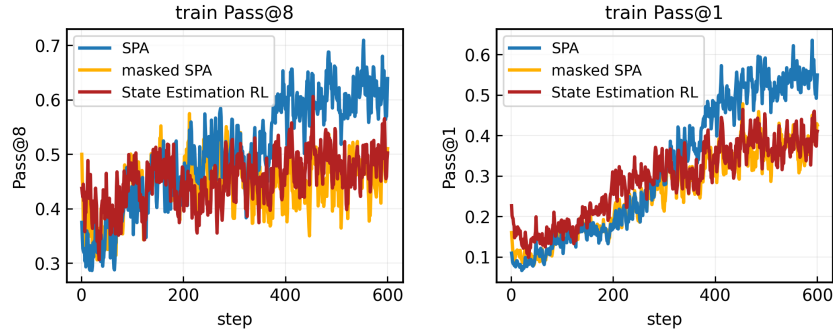


Figure 4: RL performance after world-modeling SFT under three settings: State Estimation RL baseline, No masking vs. Masking current states with next states for SPA.

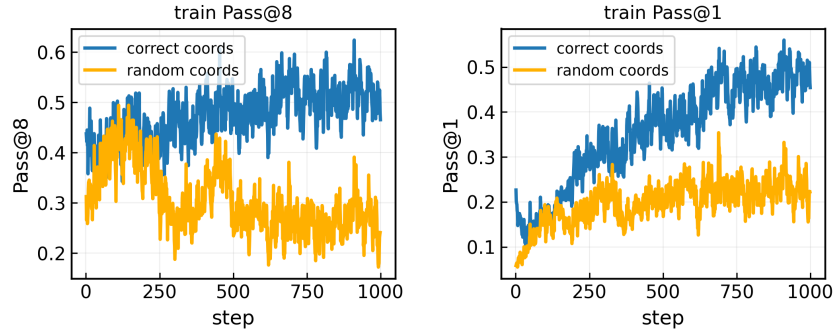


Figure 5: Pass@8 and Pass@1 comparison by using correct abstraction and incorrect abstraction on Sokoban during RL training. Left: Abstraction PPO with correct coordinates. Right: randomized coordinates (mis-specified abstraction).

setting, SFT yields no improvement for PPO. This suggests that PPOs scaling benefits derive from transition-model learning, highlighting our world-model encoding stage as pivotal to the performance.

What happens if SFT relies solely on self-belief states rather than ground-truth states? To test whether ground-truth states are necessary, we train SFT using only the models self-belief states (i.e., without ground-truth supervision). This variant fails to improve and in fact degrades RL performance (Table 3), indicating that accurate world modelling during SFT—not merely adding a state-prediction signal—is necessary for downstream gains.

Without State Estimation, the world modelling SFT could also boost the performance. To verify whether the world-modelling SFT also boosts RL performance without State Estimation, we use a similar observation-then-prediction prompt to generate self-play data from raw symbolic states. We observe a performance gain, as shown in Table 4. We observe that SPA improves RL performance even without explicit state estimation, indicating that world-model SFT transfers effectively to the policy model.

4.2 EFFECT OF GROUND TRUTH

Ground-truth coordinates are critical for RL training. To test whether the abstract state format alone is sufficient, we hold the text template and training recipe fixed and replaced all ground-truth (x, y) coordinates (player/box/goal) with i.i.d. random coordinates drawn from the same grid at each step. This preserves the correct format but modifies the content. In Figure 5, under this random-coordinates variant, the training collapses: Pass@1 and Pass@8 stagnate at low levels with

Table 3: We replace the self-play SFT data generator with a random-action generator and compare its performance with SPA.

Method	Pass@1	Pass@8
Vanilla RL	25.6	34.0
State Estimation RL	52.7	53.9
SPA	59.8	69.5
SPA (w/ self-belief SFT)	39.2	44.2

Table 4: SPA without the State Estimation and compare with the baselines.

Method	Pass@1	Pass@8
Vanilla RL	25.6	34.0
SPA w/o S Estimation	36.3	40.6

Table 5: We replace the self-play SFT data generator with a random-action generator and compare its performance with SPA.

Method	Pass@1	Pass@8
Vanilla RL	25.6	34.0
State Estimation RL	52.7	53.9
SPA (with 1 epoch SFT)	29.2 <small>↓23.5</small>	52.7 <small>↓1.2</small>
SPA (with 5 epoch SFT)	59.8 <small>↑7.1</small>	69.5 <small>↑16.6</small>
SPA (with 1 epoch RandSFT)	0.14 <small>↓52.7</small>	0.39 <small>↓53.5</small>
SPA (with 5 epoch RandSFT)	20.2 <small>↓32.5</small>	50.0 <small>↓3.9</small>

fluctuation, whereas with correct coordinates, both metrics improve steadily. It shows that coordinates carry indispensable supervision for spatial grounding and credit assignment; without them, the policy cannot align with actionable spatial relations, leading to brittle exploration and poor generalization.

4.3 EFFECT OF INITIAL POLICY FOR EXPLORATION

Can the RL policy be replaced with random actions for generating world-modeling trajectories? We realize that world-modeling trajectories need not be collected exclusively with the learned policy; they can also be obtained via generic action generators. To ablate SPA, we replace its SFT data generator with a randomaction generator: at each step, we sample uniformly from the action space Up, Down, Left, Right and substitute a fixed reasoning token sequence (*I will push the box to the target.*) As shown in Table 5, trajectories produced by this random policy yield substantially worse downstream RL performance, suggesting that a prior-aware policy for self-play data collection is crucial for effective world-model training to empower the subsequent RL training.

What can we do to enable effective exploration when the policy model is weak? We find that many failures originate from instruction noncompliance during data generation: some models fail to follow the specified output format, preventing reliable synthesis of world-modeling samples. To quantify this effect, we conduct an ablation comparing performance before and after filtering out SFT samples that deviate from the required format. Building on this, we evaluate three settings under the same RL budget on the LLaMA-3.2-1B-Instruct model in the Sokoban environment: **Original SFT**, which distills world-state transitions via supervised learning; **Filtered SFT**, where the data samples are cleaned by enforcing minimal structural validity (<observation><prediction> reasoning followed by an <answer>); and **Abs PPO**, where PPO is trained on raw grids enriched by abstraction, without transition-model SFT. As shown in Figure 8, removing misaligned data improves training stability and yields clear gains (e.g., higher Pass@k and Pass@1), indicating that strict format adherence is critical for learning accurate state and transition structure.

4.4 EFFECT OF EXTENDED SFT

To investigate the impact of spending more compute on world-modeling SFT, we vary the length of SFT from 1 to 5 epochs, and perform RL on all 5 checkpoints under the same setup. Figure 6 shows the final performance after 1000 steps of RL training. As the world model is trained longer, downstream RL improves consistently: Pass@1 rises from 0.29 to 0.60 and Pass@k from 0.53 to 0.70. Efficiency also improves: the average number of actions per episode decreases from 8.47 to 6.44, while action effectiveness rebounds from an early dip at Epoch 2’s 0.60 to 0.77 by Epoch 5. Response length climbs from 65 tokens at Epoch 1 and then stabilizes in the 160 to 175 range for Epochs 2–5, indicating that gains are not caused by verbosity but by better spatial grounding and transition prediction. Overall, longer world-model SFT supplies a stronger dynamics prior and clearer state representations, yielding higher success and shorter trajectories under the same RL budget.

5 FINDINGS: EXPLORATION, EXPLOITATION, AND GENERALIZATION

In this section, we examine both the in-domain training dynamics and the out-of-domain generalization of our method, and we find that multi-turn RL reveals a distinctive exploration-exploitation trajectory and easy2hard SPA could work well. And the trained agents could generalize to higher task complexities within the same environment family, though it fails to transfer across games with fundamentally different dynamics.

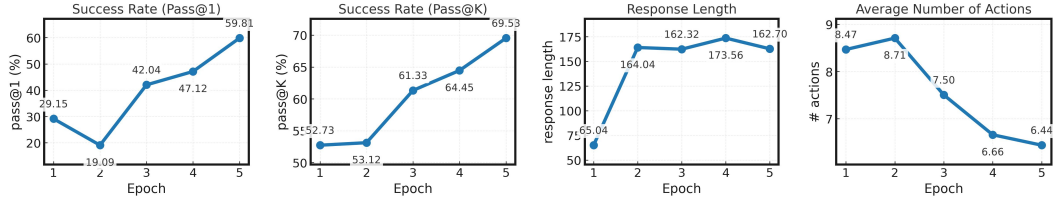


Figure 6: We evaluate RL training under initializations with varying SFT epochs and observe that increasing world-modeling SFT generally improves subsequent RL performance.

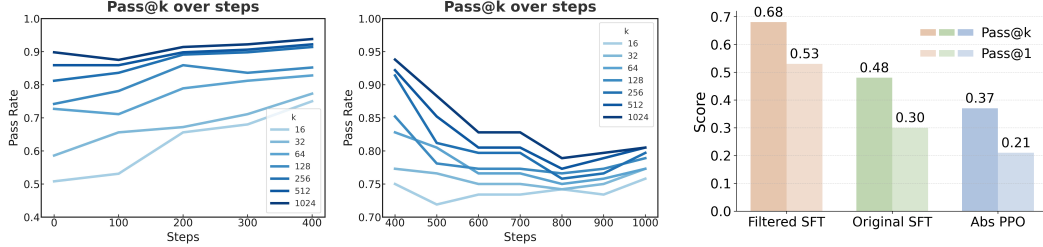


Figure 7: Pass@k performance on Sokoban during RL training. Left: steps 0–400, Pass@k consistently rises (exploration). Right: steps 400–1000, Pass@k declines as k increases (exploitation). Even at $k=1024$, early exploration improves success rates, contrasting with RLVR findings in the math domain.

Figure 8: Results on Sokoban with LLaMA under three settings: Filtered SPA SFT, raw data SPA SFT and State Estimation PPO.

Environment interaction expands reasoning frontiers. By enabling direct environment interaction, multi-turn RL broadens the reasoning frontier. Prior work (Yue et al., 2025) shows that RL with Verifiable Rewards (RLVR) improves sampling efficiency toward correct solutions but does not yield fundamentally new reasoning strategies. Moreover, RLVR exhibits a crossover in performance: RLVR-trained models outperform their base counterparts at small k (e.g., $k=1$), while base models achieve higher Pass@k at large k . In contrast, our multi-turn setting displays no such reversal. As shown in Figure 7, Pass@k continues to increase in the early phase of training (steps 0–400), remaining high even at $k=1024$, and only decreases during the later phase (steps 400–1000). This trajectory reflects an exploration-then-exploitation dynamic of the policy, highlighting the necessity of environment exploration and explaining the discrepancy from math-domain RLVR results.

World-modeling enables easy-to-hard transfer gains. We investigate whether world modeling learned in a low-complexity setting can generalize to a more complex setting and thereby accelerate further RL training. Concretely, we train the world model with SFT on the simple FrozenLake environment (grid size 4×4) and then deploy it to boost RL on the more challenging variant (6×6). As shown in Figure 9, the proposed easy-to-hard transfer substantially outperforms all non-world-modeling baselines, yielding faster learning and higher asymptotic returns. These results provide direct evidence that learning simple world dynamics can serve as a reusable prior that generalizes to more complex settings, boosting sample efficiency and policy quality in harder tasks.

Generalization across games and complexity levels. We further examine whether the trained game agents could generalize beyond its training setting. Table 6 reports two evaluation protocols. In the *cross-complexity* setting, SPA is trained on a simple Sokoban variant (6×6 grid, one box) and tested on a more complex variant (10×10 grid, two boxes). SPA outperforms a baseline trained directly on the complex task, indicating that world-model SFT facilitates scaling to higher task complexity within the same environment family. In the *cross-game* setting, SPA trained on Sokoban is evaluated on FrozenLake environment, indicating that cross-game generalization is difficult.

6 RELATED WORK

OOD scenarios for LLMs. Large language models (LLMs) (Achiam et al., 2023; Team, 2024) have advanced from static knowledge bases to versatile agents capable of planning (Cao et al., 2025), tool use (Schick et al., 2023), and multi-step reasoning (DeepSeek-AI et al., 2025). Despite these strengths, their effectiveness is largely constrained by the pre-training distribution and degrades when

Table 6: Results of cross-complexity and cross-game generalization experiments. The upper two rows are cross-complexity, and the lower two rows are cross-game generalization. We see that trained agents can generalize to harder environments but not to other environments.

Evaluation setting	Pass@1 (%)	Pass@k (%)
Simple → Complex (Sokoban)	0.9	3.1
Complex (Sokoban, baseline)	0.1	0.8
Sokoban → FrozenLake	15.9	49.2
FrozenLake (baseline)	17.2	49.2

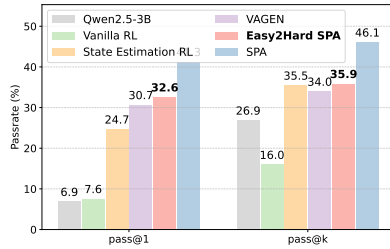


Figure 9: Results of easy-to-hard SPA on FrozenLake. Easy2Hard SPA surpasses all non-world-model baselines and VAGEN, trailing SPA trained on the target complexity.

deployed in out-of-distribution (OOD) agents environments such as robotics (Szot et al., 2023), game playing (Shao et al., 2019), and web automation (Ning et al., 2025). These domains often involve stochastic dynamics, partial observability, and task-specific rules. Without explicit grounding in environment states, LLMs struggle to learn reliable state-conditioned policies (Xing et al., 2025), resulting in fragile or sub-optimal behavior. This grounding gap remains a fundamental limitation for deploying LLM agents in real-world, interactive scenarios.

Agent Pipeline and Training. To address this challenge, prior Agent work has primarily focused on prompting-based frameworks (Yao et al., 2023; Shinn et al., 2023; Topsakal & Akinci, 2023) and reinforcement learning pipelines (Song et al., 2024; Wang et al., 2025b). These approaches typically follow a short-horizon “think-then-act” paradigm, generating actions autoregressively without an internal mechanism to persist or simulate environment dynamics. In contrast, classical RL has shown the benefits of explicit world models: latent state representations and transition modeling enable stronger credit assignment, more effective planning, and higher sample efficiency (Janner et al., 2019; Yu et al., 2020). Inspired by this model-based perspective, we argue that LLM agents can similarly benefit from an internal world model. By jointly learning state estimations and transition modeling, agents can better simulate long-term consequences of actions, thereby bridging the gap between language-based reasoning and grounded policy learning. Recent work Wang et al. (2025a) introduces an online world modeling method during RL via reward shaping, which is closely related to us.

7 CONCLUSION & LIMITATIONS

LLM agents often fail to improve Pass@k in OOD environments, reflecting a reliance on memorized trajectories rather than reasoning over environment dynamics. This limitation stems from the absence of a world model that can infer world states from observations and predict future transitions. We introduce SPA, which equips agents with an internal world model by combining structured state representations with a supervised transition model and subsequent reinforcement learning via PPO. Across Sokoban, FrozenLake, and Sudoku, it outperforms prompting-based, PPO-only, and reward-grounding baselines, demonstrating that explicit world modeling middle training provides stronger dynamics priors for downstream learning. Limitations remain in stochastic settings, where training stability is fragile and instruction-following errors can compromise data quality. Future work may incorporate uncertainty-aware transitions and scale to richer modalities. SPA provides a minimal and reproducible backbone for model-based agents operating in broader interactive domains.

CREDITS AND CONTRIBUTIONS

Shiqi Chen Initiated and led the project; conducted early exploration and defined the core method and codebase; implemented the training pipeline; ran main experiments for the 1.5B and 3B models; designed and executed all ablation and analysis experiments (Sec. 4.1, Sec. 4.2, Sec. 4.3.1, Sec. 5.1); wrote the manuscript and produced most figures.

Tongyao Zhu Contributed to discussions; proposed the data filtering idea in analysis; ran GPT-OSS evaluation; conducted pass@k experiments for ALFWORLD and WEBSHOP (Figure 1); performed PPL experiments; polished the manuscript.

Zian Wang Contributed to discussions; ran main experiments for the 0.5B and LLaMA-1B models; executed experiments in Sec. 4.3.2 and Sec. 5.3; conducted training on WEBSHOP; drafted Sec. 6, Sec. 7; created several figures.

Jinghan Zhang Contributed to discussions and early exploration; executed experiments in Sec. 4.3.2, Sec. 4.4, and Sec. 5.2; produced baseline results; created several figures; polished the manuscript and figures.

Kangrui Wang Contributed to discussions; proposed the coordinate-based idea; polished the manuscript.

Siyang Gao Contributed to discussions and proofreading.

Yee Whye Teh Held bi-weekly meetings with Shiqi; provided paper comments and discussions; proposed the two-stage framework and several ablation experiment ideas.

Teng Xiao Discussed the overall direction and initial idea; Discussed with Shiqi on the iterative update approach and experimental settings; revised the abstract and introduction; finalized the method section and equations.

Junxian He Held bi-weekly meetings with Shiqi; provided paper comments and discussions; proposed the random-guess PPL analysis and additional ablation experiments.

Manling Li Held bi-weekly meetings with Shiqi; provided paper comments and discussions; discussed early world model ideas with Shiqi; revised the abstract and introduction.

ACKNOWLEDGMENTS

We thank Zihan Wang, the lead author of RAGEN, for numerous insightful suggestions on this project and for sharing technical details of the RAGEN codebase. We also thank Zichen Liu for helpful suggestions on cross-game generalization evaluations, and Chang Ma, Wei Liu, Junteng Liu and Zhengyu Chen for valuable discussions. We also thank Shuaicheng Niu for pointing out some typos of the draft. YWT is supported by the Ministry of Digital Development and Information (MDDI) under the Singapore Global AI Visiting Professorship Program (Award No. AIVP-2024-002).

REFERENCES

Josh Achiam, Steven Adler, Sandhini Agarwal, Lama Ahmad, Ilge Akkaya, Florencia Leoni Aleman, Diogo Almeida, Janko Altenschmidt, Sam Altman, Shyamal Anadkat, et al. Gpt-4 technical report. *arXiv preprint arXiv:2303.08774*, 2023.

Pengfei Cao, Tianyi Men, Wencan Liu, Jingwen Zhang, Xuzhao Li, Xixun Lin, Dianbo Sui, Yanan Cao, Kang Liu, and Jun Zhao. Large language models for planning: A comprehensive and systematic survey. *arXiv preprint arXiv:2505.19683*, 2025.

DeepSeek-AI, Dong Guo, Dian Yang, Hao Zhang, et al. Deepseek-r1: Incentivizing reasoning capability in llms via reinforcement learning. *arXiv preprint arXiv:2501.12948*, 2025. URL <https://arxiv.org/abs/2501.12948>.

Abhimanyu Dubey, Abhinav Jauhri, Abhinav Pandey, Abhishek Kadian, Ahmad Al-Dahle, Aiesha Letman, Akhil Mathur, Alan Schelten, Amy Yang, Angela Fan, et al. The llama 3 herd of models. *arXiv e-prints*, pp. arXiv–2407, 2024.

Michael Janner, Justin Fu, Marvin Zhang, and Sergey Levine. When to trust your model: Model-based policy optimization. *Advances in neural information processing systems*, 32, 2019.

Bowen Jin, Hansi Zeng, Zhenrui Yue, Jinsung Yoon, Sercan Arik, Dong Wang, Hamed Zamani, and Jiawei Han. Search-r1: Training llms to reason and leverage search engines with reinforcement learning. *arXiv preprint arXiv:2503.09516*, 2025.

Liangbo Ning, Ziran Liang, Zhuohang Jiang, Haohao Qu, Yujuan Ding, Wenqi Fan, Xiao-yong Wei, Shanru Lin, Hui Liu, Philip S Yu, et al. A survey of webagents: Towards next-generation ai agents for web automation with large foundation models. In *Proceedings of the 31st ACM SIGKDD Conference on Knowledge Discovery and Data Mining* V. 2, pp. 6140–6150, 2025.

OpenAI. gpt-oss-120b & gpt-oss-20b model card, 2025. URL <https://arxiv.org/abs/2508.10925>.

Timo Schick, Jane Dwivedi-Yu, Roberto Dessì, Roberta Raileanu, Maria Lomeli, Eric Hambrø, Luke Zettlemoyer, Nicola Cancedda, and Thomas Scialom. Toolformer: Language models can teach themselves to use tools. *Advances in Neural Information Processing Systems*, pp. 68539–68551, 2023.

John Schulman, Filip Wolski, Prafulla Dhariwal, Alec Radford, and Oleg Klimov. Proximal policy optimization algorithms. *arXiv preprint arXiv:1707.06347*, 2017.

Kun Shao, Zhentao Tang, Yuanheng Zhu, Nannan Li, and Dongbin Zhao. A survey of deep reinforcement learning in video games. *arXiv preprint arXiv:1912.10944*, 2019.

Noah Shinn, Federico Cassano, Edward Berman, Ashwin Gopinath, Karthik Narasimhan, and Shunyu Yao. Reflexion: Language agents with verbal reinforcement learning, 2023.

Yifan Song, Da Yin, Xiang Yue, Jie Huang, Sujian Li, and Bill Yuchen Lin. Trial and error: Exploration-based trajectory optimization of LLM agents. In Lun-Wei Ku, Andre Martins, and Vivek Srikumar (eds.), *Proceedings of the 62nd Annual Meeting of the Association for Computational Linguistics (Volume 1: Long Papers)*, pp. 7584–7600, Bangkok, Thailand, August 2024. Association for Computational Linguistics. doi: 10.18653/v1/2024.acl-long.409. URL <https://aclanthology.org/2024.acl-long.409/>.

Andrew Szot, Max Schwarzer, Harsh Agrawal, Bogdan Mazoure, Walter Talbott, Katherine Metcalf, Natalie Mackraz, Devon Hjelm, and Alexander Toshev. Large language models as generalizable policies for embodied tasks. *arXiv preprint arXiv:2310.17722*, 2023.

Qwen Team. Qwen2.5: A party of foundation models, September 2024. URL <https://qwenlm.github.io/blog/qwen2.5/>.

Oguzhan Topsakal and Tahir Cetin Akinci. Creating large language model applications utilizing langchain: A primer on developing llm apps fast. In *International conference on applied engineering and natural sciences*, volume 1, pp. 1050–1056, 2023.

Kangrui Wang, Pingyue Zhang, Zihan Wang, Yaning Gao, Linjie Li, Qineng Wang, Chi Wan, Hanyang Chen, Yiping Lu, Zhengyuan Yang, Lijuan Wang, Ranjay Krishna, Jiajun Wu, Li Fei-Fei, Yejin Choi, and Manling Li. VAGEN: Reinforcing world model reasoning for multi-turn vlm agents. In *Advances in Neural Information Processing Systems*. NeurIPS, 2025a.

Zihan Wang, Kangrui Wang, Qineng Wang, Pingyue Zhang, Linjie Li, Zhengyuan Yang, Xing Jin, Kefan Yu, Minh Nhat Nguyen, Licheng Liu, et al. Ragen: Understanding self-evolution in llm agents via multi-turn reinforcement learning. *arXiv preprint arXiv:2504.20073*, 2025b.

Jialong Wu, Baixuan Li, Runnan Fang, Wenbiao Yin, Liwen Zhang, Zhengwei Tao, Dingchu Zhang, Zekun Xi, Gang Fu, Yong Jiang, et al. Webdancer: Towards autonomous information seeking agency. *arXiv preprint arXiv:2505.22648*, 2025.

Eric Xing, Mingkai Deng, Jinyu Hou, and Zhiting Hu. Critiques of world models, 2025. URL <https://arxiv.org/abs/2507.05169>.

Shunyu Yao, Jeffrey Zhao, Dian Yu, Nan Du, Izhak Shafran, Karthik Narasimhan, and Yuan Cao. ReAct: Synergizing reasoning and acting in language models. In *International Conference on Learning Representations (ICLR)*, 2023.

Tianhe Yu, Garrett Thomas, Lantao Yu, Stefano Ermon, James Y Zou, Sergey Levine, Chelsea Finn, and Tengyu Ma. Mopo: Model-based offline policy optimization. *Advances in Neural Information Processing Systems*, 33:14129–14142, 2020.

Yang Yue, Zhiqi Chen, Rui Lu, Andrew Zhao, Zhaokai Wang, Shiji Song, and Gao Huang. Does reinforcement learning really incentivize reasoning capacity in llms beyond the base model? *arXiv preprint arXiv:2504.13837*, 2025.

A PROMPTS

Sokoban Prompt: Base mode

You are solving the Sokoban puzzle.
 You are the player and you need to push all boxes to targets.
 You are provided with a symbol grid and the zero-indexed coordinates of the player, each box, and each target.
 Coordinates range from the top-left corner (0, 0) to the bottom-right corner (5, 5).
 When you are exactly next to a box, you can push it by moving in the same direction.
 You cannot push a box through a wall, and you cannot pull a box.
 The answer should be a sequence of actions, like <answer>Right || Right || Up</answer>.

Sokoban Prompt: Observation then prediction

You are solving the Sokoban puzzle.
 You are the player and you need to push all boxes to targets.
 You are provided with a symbol grid and the zero-indexed coordinates of the player, each box, and each target.
 Coordinates range from the top-left corner (0, 0) to the bottom-right corner (5, 5).
 When you are exactly next to a box, you can push it by moving in the same direction.
 You cannot push a box through a wall, and you cannot pull a box.
 The answer should be a sequence of actions, like <answer>Right || Right || Up</answer>.

A sample full output is as follows:
 <think>
 <observation>
 #####
 #_###
 #_P##
 #_X#_
 #_O_
 #####
 Player (P) is at (2,2); box (X) is at (3,2); target (O) is at (4,3).
 </observation>
 1 Down - I push box to (4,2).
 2 Left - I step to (3,1).
 3 Down - I stand left of box, ready to push it Right onto target.
 <prediction>
 #####
 #_###
 #_##
 #_#_
 #P#O_
 #####
 </prediction>
 </think>
 <answer> Down || Left || Down </answer>

FrozenLake Prompt: Base mode

You are solving the FrozenLake puzzle.
 Forbid the whole and go to the target.
 You may move to the unintended direction due to the slippery ice.
 Example answer format:
 <think>To forbid the hole and go to the target, I should go left then go up.
 </think>
 <answer>Left || Up</answer>

FrozenLake Prompt: Observation then prediction

You are solving the FrozenLake puzzle.
 Forbid the whole and go to the target.
 You may move to the unintended direction due to the slippery ice.
 Example answer format:
 <think>To forbid the hole and go to the target, I should go left then go up.
 </think>
 <answer>Left || Up</answer>

A sample full output is as follows:

```
<think>
<observation>
_0_-
0___
G___
__P_
</observation>
Player at (3,2); holes at (0,1) and (1,0); goal at (2,0). 1 Up move to safe ice
(2,2). 2 Left slide to (2,1), adjacent to goal. 3 Left reach goal (2,0);
player now on G.
<prediction>
_0_-
0___
√___
_____
</prediction>
</think>
<answer> Up || Left || Left </answer>"
```

Sudoku Prompt: Base mode

You are solving 4x4 Sudoku.
 Fill empty cells with digits 14.
 Use a 1-indexed grid (rows/cols start at 1).
 A move is exactly: row,col,value (three integers).
 In one turn you may output multiple moves, separated by ||.
 Only propose moves that keep the row, column, and 2x2 subgrid valid. Always
 output EXACTLY as:
 <think>[brief reasoning]</think>
 <answer>[r,c,v || r,c,v ...]</answer>
 No extra text outside the two tags.
 Keep the response under 50 words.
 Example:
 <think>Row 1 has one empty cell place 1. Column 2 then needs 2.
 </think>
 <answer>1,3,1 || 3,2,2</answer>

Sudoku Prompt: Observation then prediction

You are solving 4x4 Sudoku.
 Fill empty cells with digits 1-4.
 Use a 1-indexed grid (rows/cols start at 1).
 A move is exactly: row,col,value (three integers).
 In one turn you may output multiple moves, separated by ||.
 Only propose moves that keep the row, column, and 2x2 subgrid valid. Always
 output EXACTLY as:
 <think>[brief reasoning]</think>
 <answer>[r,c,v || r,c,v ...]</answer>
 No extra text outside the two tags.
 Keep the response under 50 words.

An example output:
 <think>
 <observation>
 | . . 1 4 | 1 4 . 3 | 4 2 . . | . 1 4 2
 Empty positions to be filled are at (1,1), (1,2), (2,3), (3,3), (3,4), (4,1)
 </observation>
 <prediction>
 | 2 3 1 4 | 1 4 2 3 | 4 2 3 1 | . 1 4 2
 Empty positions to be filled are at (4,1)
 </prediction>
 </think>
 <answer> 1,1,2 || 1,2,3 || 2,3,2 || 3,3,3 || 3,4,1 </answer>.

B EXPERIMENTAL SETUP

Experiments run on up to 8×80 G NVIDIA H100. For training, we instruction-tune on 1280 samples using AdamW with learning rate 1×10^{-4} . We apply PPO initialized from the SFT checkpoint, using a learning rate of 1×10^{-6} for actor and 1×10^{-5} for critic. It takes about 12 hours on single GPU to train Qwen2.5-1.5B-Instruct for 1,000 steps. For evaluation, we report decoding-only results with temperature 1.0, top- p 1.0, and max new tokens 400. Upon acceptance, we will release code, configuration files, and trained checkpoints.

C FULL RESULTS

Table 7 reports the complete results. We also include the performance before RL training (step = 0) for both settings: (i) StateEstimation PPO, evaluated with the StateEstimation prompt, and (ii) SPA immediately after the worldmodeling SFT stage. At step 0, the StateEstimation prompt yields better performance than baseline, whereas the additional worldmodeling SFT slightly lowers accuracy. However, after subsequent RL training, SPA quickly recovers and ultimately surpasses StateEstimation PPO across tasks, indicating that the structure learned during SFT provides a transferable inductive bias that RL can exploit for better generalization.

D USE OF LARGE LANGUAGE MODELS (LLMs)

During the preparation of this paper, we used large language models (LLMs) such as ChatGPT for assistance in polishing the writing and improving the clarity of figures. LLMs were not used for research ideation, experimental design, or the production of experimental results. All conceptual contributions, analyses, and conclusions are solely those of the authors. The authors take full responsibility for the content of this paper.

Table 7: Results on Sokoban, FrozenLake, and Sudoku for different models. (Metrics in $\times 10^{-2}$).

Model	Sokoban		FrozenLake		Sudoku	
	Pass@1	Pass@8	Pass@1	Pass@8	Pass@1	Pass@8
Qwen2.5-0.5B-Instruct	5.5	25.8	8.1	32.8	0.0	0.0
PPO	16.9	35.9	22.8	30.1	0.0	0.0
+State Estimation	5.2	25.4	6.7	28.5	0.1	0.8
+State Estimation RL	20.4	38.7	24.2	26.6	4.5	14.1
+ SPA SFT	1.8	11.7	3.1	15.6	0.1	0.8
+ SPA	36.7	45.3	46.9	65.6	18.2	43.8
+VAGEN	33.3	44.9	25.8	40.6	0.1	0.8
Qwen2.5-1.5B-Instruct	16.3	47.3	17.2	49.2	1.6	11.3
PPO	25.6	34.0	22.1	30.7	0.0	0.0
+State Estimation	15.7	43.8	18.6	51.2	0.3	2.3
+State Estimation RL	52.7	53.9	27.6	34.8	39.1	72.3
+ SPA SFT	8.3	36.7	9.8	43.8	3.5	24.2
+ SPA	59.8	69.5	70.9	75.0	59.6	94.9
+VAGEN	44.5	50.0	37.7	43.0	0.0	0.0
Qwen2.5-3B	12.5	35.9	6.9	26.9	0.0	0.0
PPO	31.4	35.5	7.6	16.0	0.0	0.0
+State Estimation	9.9	39.3	6.9	26.6	0.1	0.8
+State Estimation RL	26.2	27.7	24.7	35.5	24.1	26.2
+ SPA SFT	6.0	29.7	1.6	10.5	0.3	2.7
+ SPA	49.7	58.2	41.3	46.1	69.9	89.8
+VAGEN	31.9	43.0	30.7	34.0	0.0	0.0
LLaMA3.2-1B-Instruct	8.3	33.2	10.2	41.0	0.0	0.0
PPO	21.2	39.8	10.8	24.6	0.1	1.2
+State Estimation	9.6	33.6	10.9	43.0	0.1	0.8
+State Estimation RL	31.6	44.1	19.3	29.7	45.0	71.1
+ SPA SFT	6.3	27.7	11.4	38.3	1.3	9.8
+ SPA	53.0	68.0	64.8	71.1	81.3	100
+VAGEN	47.4	50.8	24.5	29.3	0.1	0.8
GPT-OSS-20B	45.8	84.4	68.8	100	61.8	100
+State Estimation	55.1	89.1	73.3	100	68.1	100